

Published in final edited form as:

*Cancer Discov*. 2012 November ; 2(11): 1036–1047. doi:10.1158/2159-8290.CD-11-0348.

# PI3K Inhibition Impairs BRCA1/2 Expression and Sensitizes BRCA-Proficient Triple-Negative Breast Cancer to PARP Inhibition

**Yasir H. Ibrahim**[1], **Celina García-García**[1], **Violeta Serra**[1], **Lei He**[6,7], **Kristine Torres-Lockhart**[6], **Aleix Prat**[5], **Pilar Anton**[1], **Patricia Cozar**[1], **Marta Guzmán**[1], **Judit Grueso**[1], **Olga Rodríguez**[1], **Maria Teresa Calvo**[1], **Claudia Aura**[2], **Orland Díez**[4], **Isabel T. Rubio**[3], **José Pérez**[4], **Jordi Rodón**[4], **Javier Cortés**[4], **Leif W. Ellisen**[6,7], **Maurizio Scaltriti**[6,7], and **José Baselga**[1,6,7]

[1]Experimental Therapeutics Laboratory, Vall d'Hebron Institute of Oncology (VHIO), Pg Vall d'Hebron, Barcelona, Spain

[2]Molecular Pathology, Vall d'Hebron Institute of Oncology (VHIO), Pg Vall d'Hebron, Barcelona, Spain

[3]Breast Surgical Oncology, Vall d'Hebron Institute of Oncology (VHIO), Pg Vall d'Hebron, Barcelona, Spain

[4]Medical Oncology, Vall d'Hebron Institute of Oncology (VHIO), Pg Vall d'Hebron, Barcelona, Spain



**Corresponding Authors:** José Baselga, Massachusetts General Hospital Cancer Center, 10 North Grove Street, LRH-1, Boston, MA 02114. Phone: 617-726-2408; Fax: 617-643-9686; jbaselga@partners.org; and Maurizio Scaltriti, Massachusetts General Hospital Cancer Center, Harvard Medical School, CNY 149, 13th Street, Charlestown, MA 02129. Phone: 617-643-8239; Fax: 617-724-7298; mscaltriti@partners.org.

**Disclosure of Potential Conflicts of Interest**

J. Cortés has honoraria from the speakers' bureaus of Roche, Teva, and Ferrer and is a consultant/advisory board member of Roche, Novartis, and Celgene. J. Baselga has consulted for Novartis Pharmaceuticals, which is developing NVP-BKM120 for cancer treatment. No potential conflicts of interest were disclosed by the other authors.

The Editor-in-Chief of *Cancer Discovery* (J. Baselga) is an author of this article. In keeping with the AACR's Editorial Policy, the paper was peer reviewed and a member of the AACR's Publications Committee rendered the decision concerning acceptability.

**Authors' Contributions**

**Conception and design:** Y.H. Ibrahim, C. García-García, V. Serra, L. He, L.W. Ellisen, M. Scaltriti, J. Baselga

**Development of methodology:** Y.H. Ibrahim, C. García-García, V. Serra, L. He, K. Torres-Lockhart, P. Anton, P. Cozar, O. Rodríguez, M.T. Calvo, J. Cortés

Acquisition of data (provided animals, acquired and managed patients, provided facilities, etc.): Y.H. Ibrahim, C. García-García, V. Serra, L. He, K. Torres-Lockhart, P. Anton, P. Cozar, M. Guzmán, J. Grueso, O. Rodríguez, M.T. Calvo, O. Díez, I.T. Rubio, J. Péréz, J. Rodón, J. Cortés

Analysis and interpretation of data (e.g., statistical analysis, biostatistics, computational analysis): Y.H. Ibrahim, C. García-García, V. Serra, L. He, K. Torres-Lockhart, C. Prat, M. Guzmán, O. Díez, I.T. Rubio, J. Rodón, J. Cortés, L.W. Ellisen, M. Scaltriti, J. Baselga

Writing, review, and/or revision of the manuscript: Y.H. Ibrahim, C. García-García, V. Serra, L. He, K. Torres-Lockhart, A. Prat, J. Rodón, J. Cortés, L.W. Ellisen, M. Scaltriti, J. Baselga

Administrative, technical, or material support (i.e., reporting or organizing data, constructing databases): Y.H. Ibrahim, C. García-García, V. Serra, L. He, K. Torres-Lockhart, C. Aura, J. Péréz, J. Cortés, M. Scaltriti

**Study supervision:** Y.H. Ibrahim, C. García-García, V. Serra, M. Scaltriti, J. Baselga

**Note:** Supplementary data for this article are available at Cancer Discovery Online (http://cancerdiscovery.aacrjournals.org/).

[5]Lineberger Comprehensive Cancer Center, University of North Carolina, Chapel Hill, North Carolina

[6]Massachusetts General Hospital Cancer Center, Massachusetts General Hospital

[7]Harvard Medical School, Boston, Massachusetts

## Abstract

PARP inhibitors are active in tumors with defects in DNA homologous recombination (HR) due to *BRCA1/2* mutations. The phosphoinositide 3-kinase (PI3K) signaling pathway preserves HR steady state. We hypothesized that in BRCA-proficient triple-negative breast cancer (TNBC), PI3K inhibition would result in HR impairment and subsequent sensitization to PARP inhibitors. We show in TNBC cells that PI3K inhibition leads to DNA damage, downregulation of BRCA1/2, gain in poly-ADP-ribosylation, and subsequent sensitization to PARP inhibition. In TNBC patient–derived primary tumor xenografts, dual PI3K and PARP inhibition with BKM120 and olaparib reduced the growth of tumors displaying BRCA1/2 downregulation following PI3K inhibition. PI3K-mediated BRCA downregulation was accompanied by extracellular signal–regulated kinase (ERK) phosphorylation. Overexpression of an active form of MEK1 resulted in ERK activation and downregulation of BRCA1, whereas the MEK inhibitor AZD6244 increased BRCA1/2 expression and reversed the effects of MEK1. We subsequently identified that the ETS1 transcription factor was involved in the ERK-dependent BRCA1/2 downregulation and that knockdown of ETS1 led to increased BRCA1/2 expression, limiting the sensitivity to combined BKM120 and olaparib in 3-dimensional culture.

**SIGNIFICANCE—**Treatment options are limited for patients with TNBCs. PARP inhibitors have clinical activity restricted to a small subgroup of patients with *BRCA* mutations. Here, we show that PI3K blockade results in HR impairment and sensitization to PARP inhibition in TNBCs without *BRCA* mutations, providing a rationale to combine PI3K and PARP inhibitors in this indication. Our findings could greatly expand the number of patients with breast cancer that would benefit from therapy with PARP inhibitors. On the basis of our findings, a clinical trial with BKM120 and olaparib is being initiated in patients with TNBCs.

## INTRODUCTION

Therapeutic options for triple-negative breast cancer (TNBC) are limited and based on the use of multiple lines of chemotherapy (1). An exception to this paradigm is found in the small subset of TNBCs that have defects in homologous recombination (HR)-mediated DNA repair due to *BRCA1*/2 mutations, in which therapy with PARP inhibitors results in high antitumor activity (2–5). PARP enzymatic activity is necessary for the repair of single-strand breaks (SSB) through the base excision repair (BER) pathway. Several double-strand break repair mechanisms exist, including HR, which uses a sister chromatid template for recombination, and nonhomologous end joining, which uses DNA ligation for repair but exhibits lower fidelity than HR (5). When PARP is inhibited, unrepaired SSBs can degenerate to DSBs that, in BRCA-deficient cells, can no longer be repaired by HR, resulting in a continuous and lethal DNA damage (4–6). BRCA1 and BRCA2 proteins are essential components of HR that are recruited to damaged DNA for repair of the DSBs. Therefore, the loss of BRCA1/2 results in HR deficiency and sensitization to PARP

inhibitors. HR deficiency can also occur through other mechanisms that may promote sensitivity to PARP inhibition: (i) methylation and silencing of the Fanconi anemia genes (7), involved in DNA repair and associated with BRCA1/2, (ii) loss of CDK1 activity, which maintains BRCA1 protein stability (8), or (iii) loss of RAD51 expression (7, 9), a necessary recombinase in the HR complex that associates with BRCA1/2.

TNBCs also display aberrant activation of the phosphoinositide 3-kinase (PI3K) pathway, which occurs due to a variety of mechanisms including loss of negative pathway regulators such as PTEN or inositol polyphosphate 4-phosphatase type II (INPP4B; refs. 10, 11), activating mutations of the *PIK3CA* gene (12), or overexpression of the EGF receptor (13). Direct pharmacologic inhibition of PI3K/AKT/mTOR signaling is, therefore, an attractive clinical strategy for this disease. In addition to regulating cellular processes including metabolism, growth, and survival (14), PI3K also stabilizes and preserves DSB repair by interacting with the HR complex under normal conditions (15) and is necessary for DNA repair during ionizing radiation (16). Here, we investigate the effects of PI3K inhibition in perturbing DNA HR in preclinical models of TNBCs containing PI3K-activating alterations. We found that PI3K blockade promotes HR deficiency by downregulating BRCA1/2 and sensitizes BRCA-proficient tumors to PARP inhibition.

## RESULTS

### PI3K Suppression Impairs Homologous Recombination

TNBC is exquisitely sensitive to chemotherapy. This is due, at least in part, to intrinsic genomic instability of TNBC cells as a result of deficient DNA repair (17). Because PI3K signaling is known to maintain HR steady state (15), we asked whether inhibition of PI3K would further promote DNA damage in TNBCs. To test this hypothesis, we first used siRNA to knockdown the expression of *PIK3CA*, the gene encoding for the α-isoform of the catalytic p110 subunit of the PI3K enzyme complex, in MDA-MB-468 cells, a *BRCA* wild-type PTEN-null TNBC cell line. *PIK3CA* knockdown resulted in accumulation of phosphorylated histone 2AX (γH2AX), a protein that localizes to damaged DNA (18) and recruits DNA repair effectors to these sites (ref. 19; Fig. 1A and B). γH2AX accumulation, occurring mainly in the S- and $G_2$ phases of the cell cycle, was further enhanced by concomitant treatment with olaparib, a small-molecule PARP inhibitor. In the same assay, siRNA for *BRCA1* served as a positive control for γH2AX accumulation following PARP inhibition.

Concomitantly, we observed that suppression of *PIK3CA* was accompanied by downregulation of BRCA1, indicating that PI3K suppression *per se* can inhibit the expression of proteins necessary for HR (Fig. 1C; Supplementary Fig. S1). Importantly, *BRCA1* downregulation by itself had little effect in increasing γH2AX nuclear foci formation. Subsequently, we investigated whether pharmacologic inhibition of PI3K could recapitulate the effects on BRCA expression observed by *PIK3CA* knockdown (Fig. 1D). Consistently, treatment with a pan-PI3K inhibitor (NVP-BKM120, hereafter referred to as BKM120), resulted in decreased expression of BRCA1/2 and concomitant gain of Poly(ADP-ripose) (PAR) proteins, a product (and marker) of PARP activation (20). Quantitative real-time PCR (qRT-PCR) showed that BRCA1/2 downregulation occurred, at

least in part, at the transcriptional level and was not limited to MDA-MB-468 cells (Fig. 1E; Supplementary Fig. S2).

## HR Deficiency Induced by PI3K Suppression Sensitizes to PARP Inhibition

In the setting of decreased HR activity, PARP inhibition results in chromatid aberrations leading to cell lethality (5). To evaluate whether HR impairment following PI3K suppression conferred increased sensitivity to PARP inhibition, we tested the *in vitro* activity of 2 PARP inhibitors, olaparib (Fig. 2; Supplementary Fig. S3A) and ABT888 (Supplementary Fig. S3B), in cells transfected with *PIK3CA* siRNA or treated with BKM120. Knockdown of *PIK3CA* decreased the $IC_{50}$ for olaparib in MDA-MB-468 (Fig. 2A) and BT20 (Supplementary Fig. S3B) TNBC cells. Knockdown of *PIK3CB* also led to sensitization to olaparib or ABT888, albeit to a lesser extent (data not shown). The combination of olaparib and BKM120 was superior to single agent in inhibiting colony formation in soft agar in MDA-MB-468 cells (Fig. 2B). The superiority of the combination was observed in additional TNBC *BRCA* -wild-type cell lines (MDA-MB-231: *RAS*-mutated; HCC1143: *PTEN*-null; HCC70: PTEN-null) as well as with different PI3K inhibitors (GDC-0941; Fig. 2C).

## BKM120-Mediated BRCA Downregulation Sensitizes to PARP Inhibition in Patient-Derived Primary Tumor Xenografts

To study the effects of BKM120 in modulating BRCA expression and consequent sensitization to olaparib in models that better represent patient tumors, we decided to use 3 TNBC patient–derived tumor xenografts developed from 3 different patients with breast cancer at our institution (Table 1). These models have been reported to resemble both the morphologic and molecular characteristics of the original patient tumors from which they have been expanded (21, 22). Indeed, tissue architecture, hormone receptor levels, HER2, and PTEN expression of our xenografts were indistinguishable from their original tumors (Supplementary Fig. S4). In concordance with the high frequency of PTEN loss reported in TNBCs (12, 23), PTEN expression was barely detectable in any of the TNBC models, whereas an activating *PIK3CA* mutation (H1047R) was detected in one (TNBC1). Of note, both PTEN loss and *PIK3CA* mutations have been previously reported to coexist in breast cancer (23).

Accumulation of nuclear γH2AX foci following PI3K inhibition was variable in the 3 TNBC models (Fig. 3A). TNBC1 and TNBC3 showed a 2-fold increase in γH2AX staining, whereas no significant changes occurred in TNBC2 following BKM120 treatment. The inability of TNBC2 to accumulate γH2AX foci following PI3K inhibition may be due to its intrinsic resistance (and lack of significant cell death; refs. 24, 25) to BKM120 used as a single agent (data not shown). Downregulation of BRCA expression upon BKM120 treatment occurred in TNBC1 and TNBC2 and was accompanied by an increase in PAR levels (Figs. 3B, 3C). We therefore hypothesized that combined PI3K and PARP inhibition was likely to be effective in these 2 xenograft models. BKM120 as a single agent temporarily reduced tumor growth in TNBC1 and TNBC3 but was scarcely efficacious in TNBC2. As expected, olaparib monotherapy was ineffective in all 3 models. However, the combination of BKM120 with olaparib was superior to single agents in reducing TNBC1

and TNBC2 tumor growth (Fig. 4). Consistently, lack of BRCA downregulation and PARP activation (TNBC3; Fig. 3B and C) coincided with little or no benefit from dual PI3K and PARP suppression (TNBC3; Fig. 4).

Taken together, these results suggest that (i) the degree of HR impairment and consequent sensitization to PARP inhibition induced by PI3K blockade may vary among different TNBC populations and (ii) the sensitivity to dual PARP and PI3K treatment may be dependent on the degree of BRCA1/2 downregulation and consequent increased PARP activity (PAR) following PI3K inhibition.

## Extracellular Signal–Regulated Kinase Inhibition Prevents the BKM120-Mediated Decrease in BRCA Expression and Increase in PARP Activity

Next, we searched for possible mechanisms that could explain the variability in BRCA1/2 expression (and consequent susceptibility to PARP inhibition) following PI3K suppression. Interestingly, in both TNBC1 and TNBC2, we observed a concomitant increase of extracellular signal–regulated kinase (ERK) phosphorylation upon BKM120 treatment (Fig. 3C). This finding was not surprising as ERK activation following PI3K blockade in breast cancer has been previously described by us and others (26–28). To explore whether BRCA1/2 expression may be regulated by the ERK pathway, we undertook several approaches. First, we exogenously expressed an active form of MEK1 (thus increasing ERK phosphorylation) in MDA-MB-468 cells and asked whether elevated ERK activity *per se* led to downregulation of BRCA1. In Fig. 5A and B, we show that this in fact was the case. Moreover, pharmacologic MEK inhibition using the small-molecule MEK inhibitor AZD6244 was sufficient to increase the expression of BRCA1 and BRCA2 and reverse the effects of MEK1 overexpression.

These observations prompted us to conduct a Jaspar promoter analysis (29) searching for ERK-related transcription factors binding to either *BRCA1* or *BRCA2* promoters. This analysis identified ETS1 as the transcription factor with the highest number of *BRCA1/2* binding motifs (Supplementary Table S1). As a matter of fact, ETS transcription factors have been described to be phosphorylated (and activated) by the ERK pathway (30) and to repress the *BRCA1* promoter (31). To test whether the ETS1 transcription factor was involved in the ERK-dependent BRCA1/2 downregulation upon PI3K blockade, we measured the levels of phosphorylated ETS1 ($pETS1_{T38}$) in MDA-MB-468 cells treated with BKM120, AZD6244, and the combination of both (Fig. 5C). Together with the expected increase in ERK activation, BKM120 treatment also increased the levels of $pETS1_{T38}$ (Fig. 5C; Supplementary Fig. S5). In Fig. 5D, we confirm that PI3K suppression and ERK activation led to transcriptional *BRCA1/2* downregulation. In Fig. 5E and F, we show that these results also held true *in vivo.* In fact, TNBC1 treated with BKM120 displayed ERK activation with increased pETS1 levels that led to downregulation of BRCA1/2. This phenomenon was prevented by MEK suppression by AZD6244.

To further confirm the role of ETS1 in regulating ERK-dependent BRCA1/2 expression, we specifically knocked down *ETS1* by short hairpin RNA (shRNA) or siRNA (Fig. 6A and C; Supplementary Fig. S6) and showed that this manipulation was sufficient to increase BRCA1/2 expression and concomitantly inhibit PARP activity in 2 TNBC cell lines (Fig.

6A–D). Furthermore, *ETS1* downregulation in MDA-MB-231 cells limited the sensitivity to dual PI3K and PARP inhibition (without altering colony formation of cells treated with single agents; Fig. 6E).

Taken together, these data indicate that HR impairment following PI3K blockade may be dependent on ERK activation that in turn increases ETS1 phosphorylation (and activity) to repress BRCA1/2 expression.

## DISCUSSION

HR deficiency associated with *BRCA1*/*2* mutation results in dependence on PARP-mediated DNA repair and profound sensitivity to PARP inhibitors (2–4, 7). In contrast, the clinical activity of PARP inhibitors in non–*BRCA*-mutant tumors to date has been disappointing (32), resulting in limited applicability of these agents in the clinic. It has been proposed that somatic loss of BRCA function by promoter methylation and consequent transcriptional silencing may also induce HR deficiency, which would result in an additional fraction of patients who may potentially benefit from PARP inhibitors (33).

Our study suggests that PI3K inhibition could be exploited to induce HR deficiency and sensitization to PARP inhibition in BRCA-proficient TNBCs. Using *in vitro* models, we show that suppression of the PI3K pathway was accompanied by BRCA1/2 downregulation and an increase in PARP activity (increased PAR levels), indicating that cells undergoing PI3K suppression become more dependent on this DNA repair mechanism. As a matter of fact, dual inhibition of both PARP and PI3K activity resulted in greater suppression of cell proliferation, as well as of anchorage-independent and-dependent colony formation. However, *in vivo*, we observed that BRCA1/2 downregulation following PI3K inhibition was variable among our tested models. In those patient-derived xenografts showing BKM120-dependent BRCA downregulation, the addition of olaparib significantly suppressed tumor growth. No such effects were observed when BRCA1/2 levels remained unchanged by PI3K inhibition. This would suggest that BRCA expression rather than DNA damage following PI3K inhibition predicts response to PARP inhibition. This observation is in accordance with recent data indicating that response to chemotherapy in TNBCs occurs exquisitely in tumors with impaired BRCA nuclear expression/localization independently of the magnitude of DNA damage (34).

Intriguingly, in the tumors responding to combined therapy, BRCA1/2 downmodulation was accompanied by concomitant activation of the ERK pathway following PI3K inhibition. Moreover, the use of a MEK inhibitor prevented ERK phosphorylation and limited BRCA1/2 downregulation induced by BKM120 treatment. These results indicate that *BRCA1*/*2* gene transcription may be regulated, at least in part, by the ERK pathway. Furthermore, our data suggest that ETS1 is among the transcription factors mediating this ERK-dependent BRCA downregulation. Interestingly, it has been recently proposed that the antitumor effects of olaparib may be limited to ETS-positive tumors (35). Our study supports this conclusion and argues that ETS1-dependent ERK activation is sufficient to sensitize TNBCs to dual PI3K and PARP blockade.

The magnitude of BRCA1/2 downregulation following PI3K blockade that is needed for cancer cells to acquire sensitivity to PARP inhibitors remains to be determined. Single allelic mutation of *BRCA1* is sufficient for the induction of HR deficiency (36), suggesting that changes in (and not only complete loss) in BRCA1 or BRCA2 expression could act synergistically with PARP inhibition in abolishing tumor growth.

In summary, we show that PI3K inhibition in TNBCs results in BRCA downregulation, activation of PARP, and ultimately sensitization to PARP inhibition. Importantly, BRCA1/2 downregulation following PI3K inhibition seems to be a *conditio sine qua non* to achieve strong antitumor activity when a PARP inhibitor is combined in *BRCA* -wild-type TNBCs. Our findings provide the rationale to investigate the clinical efficacy of dual PARP and PI3K inhibition in TNBCs, an approach that could expand the fraction of patients who may benefit from PARP inhibitors.

## METHODS

### Cell Culture and Inhibitors

MDA-MB-468, MDA-MB-231, HCC70, HCC1143, and BT20 cells were obtained from the American Type Culture Collection (ATCC). Cells were tested and authenticated by ATCC (DNA fingerprinting, karyotyping, and morphology study) and additionally by Western blot and Mass Array mutational analysis in our laboratory. MDA-MB-468 cells were maintained in RPMI-1640 media supplemented with 10% FBS. MDA-MB-231 cells were maintained in ATCC-formulated Eagle's Minimum Essential Medium with 10% FBS. BT20 cells were maintained in RPMI-1640, 10% FBS, supplemented with basic minimal essential amino acids (Sigma), MEM Nonessential Amino Acids (Sigma), and porcine insulin. HCC70 and HCC1143 cells were cultured in RPMI-1640 supplemented with 10% FBS. All cell cultures were conducted at 37°C in 5% $CO_2$. Low melting temperature seaplaque agarose was purchased from Lonza. Matrigel was purchased from Invitrogen. GDC-0941, MK2206, AZD6244, and AZD2281 (olaparib) were purchased from Selleck Chemicals. ABT888 was purchased from Active Biochem. Plasmids for control and MEK1 were kindly provided by Cory Johannessen at the Broad Institute (Boston, MA). The siRNAs against human *BRCA1, PIK3CA, PIK3CB* and nontargeting control #3 are ON-TARGET-*plus* Smartpool siRNAs from Dharmacon Thermal Scientific. Lipofectamine RNAiMAX Transfection Reagent was purchased from Life Technologies. siRNA for control and *ETS1* were generated using Invitrogen siRNA sequence generator and purchased from Sigma. pTRIPZ *ETS1* shRNA lentiviral (5 clones—RHS4740-NM_005238) doxycycline-regulated vector (shRNA-*ETS1*) was purchased from OpenBiosystems.

### Flow Cytometry for γH2AX

Twenty-four hours after transfection with 50 nmol/L siRNA and RNAiMAX transfection reagent according to manufacturer's protocol, cells were treated with PARP inhibitor or vehicle control for 48 hours. Cells were then trypsinized into single-cell suspension and fixed with 1% ice-cold paraformaldehyde solution for 15 minutes, followed by incubation with 70% ethanol at −20°C overnight. Cells were permeabilized with bovine serum albumin (BSA)–T–PBS (1% BSA and 0.2% Triton X-100 in PBS) and incubated with γH2AX

antibody (BD Pharmingen, Alexa Fluor 488 Mouse anti-H2AX, pS139) at 4°C overnight. Cells were then washed, resuspended in propidium iodide (PI) staining solution, and run on FACSCalibur System (BD Biosciences). Data were analyzed with FlowJo (Tree Star, Inc.).

### Cell Viability Assay

Eighteen hours after transfection with the indicated siRNAs, cells were trypsinized and plated in 96-well plates in triplicates. Six hours later, various concentrations of olaparib or ABT888 were added. After growing for 7 days, cell viability was assessed by Cell Titer-Glo (Promega).

### Clonogenic Assay

Eighteen hours after transfection with the indicated siRNAs, cells were trypsinized and plated in 6-well plates at clonal density in triplicates. Six hours later, various concentrations of olaparib or ABT888 were added. Medium was refreshed every 4 days. After growing 14 to 18 days, cell colonies were stained with methylene blue and counted by Labworks imaging software (UVP).

### Anchorage-Dependent and -Independent Growth in 3-Dimensional Culture

A 1% seaplaque agarose media mixture was solidified in 24-well plates. A cell mixture of 0.4% agarose in media and 5,000 cells was plated on top of the 1% agarose layer. After 24 hours, cells were treated with inhibitors as indicated and media containing inhibitors were changed once per week. Images were taken at a ×10 objective.

Three-dimensional (3D) anchorage culture of breast cancer cells was conducted in 100% Matrigel. Briefly, polyhema-coated 96-well plates were coated with 25 μL of Matrigel, centrifuged, and allowed to gel at 37°C. Five thousand cells were plated on top in media containing 2% Matrigel. After 3D structures were formed (3 days), cells were treated as indicated for 7 days. Phase-contrast microscopy was used to image 3D structures.

### *Generation of* ETS1 *shRNA-Expressing MDA-MB-231*

Lentiviral pTRIPZ was generated according to manufacturer's protocol, and target MDA-MB-231 cells were infected with a pool of 5 *ETS1* shRNA viral constructs. Cells were puromycin selected for 2 weeks and then treated with or without doxycycline (20 ng/mL) for 4 days.

### Western Blots

Tumor samples were homogenized in ice-cold lysis buffer [Tris-HCl, pH 7.8, 20 mmol/L; NaCl, 137 mmol/L; EDTA, pH 8.0, 2 mmol/L; NP40 1%, glycerol 10%; supplemented with NaF, 10 mmol/L; leupeptin, 10 μg/mL; $Na_2$ $VO_4$, 200 μmol/L; phenylmethylsulfonylfluoride, 5 mmol/L; and Aprotinin (Sigma-Aldrich)]. Cell lines were also collected in ice-cold lysis buffer. Lysates were cleared by centrifugation at 13,000 rpm for 10 minutes at 4°C, and supernatants were removed and assayed for protein concentration using the Pierce BCA Protein Assay Kit (Thermo Scientific). Thirty micrograms of total lysates were resolved by SDS-PAGE and electrophoretically transferred to nitrocellulose membranes. Membranes were hybridized with the following primary antibodies: phospho-

Akt (pAkt-Ser473), phospho-Akt (pAkt-Thr308), phospho-S6 (pS6-Ser240/244), phospho-ERK (pERK-Thr202/Tyr204), and total ERK (CST); BRCA1, BRCA2, and PAR (Abcam), and phospho-ETS1 (pETS1-Thr38; Invitrogen) in 1% nonfat dry milk. Mouse and rabbit horseradish peroxidase (HRP)–conjugated secondary antibodies (Amersham Biosciences) and chicken-HRP (Abcam) were used at 1:2,000 in TBS-T/1% nonfat dry milk. Protein–antibody complexes were detected by chemiluminescence with the Immobilon Western HRP Substrate and images were captured with a Fujifilm LASS-3000 camera system.

### Quantitative Real-Time PCR

qRT-PCR was carried out using TaqMan probes from Applied Biosystems, according to the manufacturer's recommendations. Reactions were carried out in an ABI 7000 sequence detector (Perkin Elmer) and results were expressed as fold change calculated by the $\Delta C_t$ method relative to the control sample. The ribosomal subunit 18S was used as an internal normalization control.

### RNA Expression Microarray Analysis

Tumor RNA was extracted by RNeasy Mini Kit (Qiagen) according to manufacturer's instructions, and 100 ng were hybridized onto Affymetrix HuGene microarrays. Data were analyzed as previously described (37).

### Establishment of Patient-Derived Tumor Grafts in Nude Mice

Patient consent for tumor use in animals was obtained under a protocol approved by the Vall d'Hebron Hospital (Barcelona, Spain) Clinical Investigation Ethical Committee and Animal Use Committee. Tumors were subcutaneously implanted in 6-week-old female HsdCpb:NMRI-*Foxn1nu* mice (Harlan Laboratories). Animals were supplemented with 1 μmol/L estradiol (Sigma) in the drinking water. After tumor graft growth, tumor tissue was re-implanted into recipient mice, which were randomized upon implant growth.

### In Vivo *Treatment Study*

Patient-derived tumor grafts: Animals bearing patient-derived tumor grafts were randomized in groups of 6 to 8 mice per group when tumor volumes reached 100 to 200 $mm^3$. Animals were treated by oral gavage with NVP-BKM120 every 6 days (dissolved in NMP-PEG) or AZD6244 (dissolved in methylcellulose/Tween). Olaparib was resuspended for intraperitoneal administration in 10% Captisol. Tumor grafts were measured with calipers, and tumor volumes were determined using the formula: (length × $width^2$) × ($\pi$/6). At the end of the experiment, animals were sacrificed by $CO_2$ inhalation. Tumor volumes are plotted as mean ± SE.

### Immunohistochemistry and Immunofluorescence

Tumor specimens and tumor grafts were fixed immediately after biopsy or excision in a 10% buffered formalin solution for a maximum of 24 hours at room temperature before being dehydrated and paraffin embedded under vacuum conditions. For tumor grafts, tissue microarrays (TMA) were constructed including triplicate cores from each graft. TMA slides underwent deparaffinization and antigen retrieval using PT Link system (Dako) following

manufacturers' instructions. Antibodies against the following targets were from Dako: estrogen receptor (ER; 1:50), progesterone receptor (PR; prediluted), HER2 (prediluted), and PTEN (1:100) from CST. Immunohistochemical staining was conducted as follows: 4-μm sections from formalin-fixed and paraffin-embedded material were deparaffinized and hydrated. Antigen retrieval was conducted using a T/T Mega microwave system following manufacturer's instructions and Dako reagents. After peroxide blocking, slides were incubated with primary antibody, secondary antibody, and finally developed with freshly prepared 0.05% 3,3′-diaminobenzidine and counterstained with hematoxylin. Positive and negative controls were run along with the tested slides per each marker.

Immunofluoresence analysis of γH2AX in MDA-MB-468 cells was conducted on cells seeded onto coated cover slips and then transfected 24 hours later with control siRNA, *BRCA1* siRNA, or *PIK3CA* siRNA. Either vehicle control or 1 μmol/L olaparib was added to the medium 24 hours after transfection. Two days after drug treatment, cells were fixed with 3% formaldehyde, permeabilized with 0.1% Triton X-100, and blocked with 10% FBS-containing PBS medium for 1 hour. Subsequently, cells were incubated with γH2AX antibody (BD Pharmingen, Alexa Fluor 488 Mouse anti-H2AX, pS139; 1:1,000), washed, counter-stained by Hoechst 33342 to visualize the nuclei, and mounted for immunofluorescence analysis. Ten fields per sample were quantified with a threshold of 10 foci or more being considered positive.

Immunofluorescence analysis of γH2AX (Millipore, 1:100) in tumor samples was conducted on formalin-fixed, paraffin-embedded TMAs. After deparaffinization, antigen retrieval was conducted by incubation in 10 mmol/L citrate buffer, pH 6.0 (Dako), in a heated (97°C) water bath for 40 minutes. Nonspecific binding was blocked by immersing the sections in a TBS/5% BSA solution for 10 minutes. Sections were incubated with a mouse monoclonal antibody at a dilution of 1:100 for 60 minutes. Anti-mouse Alexa Fluor 568 goat anti-mouse IgG (Molecular Probes) was diluted 1:700 for 30 minutes. Sections were counterstained with 4′,6-diamidino-2-phenylindole dihydrochloride (DAPI, Vysis). All incubations were conducted at room temperature. Images were acquired using a confocal microscope and quantified by a pathologist blinded to the identity of the samples.

### Statistical Analysis

One-way ANOVA with Bonferroni post-test was done using Graph-Pad Prism (GraphPad Software). Error bars represent the SE. All experiments were repeated at least 3 times.

## Supplementary Material

Refer to Web version on PubMed Central for supplementary material.

## Acknowledgments

NVP-BKM120 was kindly provided by Emmanuelle di Tomaso and Michel Maira (Novartis Pharmaceuticals). The authors thank Cory Johannessen from the Broad Institute for sharing the MEK1 plasmid, Ana Vivancos from the Cancer Genomics group at Vall d'Hebron for providing technical support with MassArray and Sanger sequencing, and Joaquín Arribas and Joan Seoane for helpful scientific discussion.

**Grant Support**

This work was funded by a Stand Up To Cancer Dream Team Translational Cancer Research Grant, a Program of the Entertainment Industry Foundation (SU2C-AACR-DT0209 to J. Baselga), the Avon Foundation (AFG01-2010-019), the Tracey Davis Memorial Fund (L.W. Ellisen), a noncommercial research agreement with Novartis (CIBOT to J. Baselga), and FERO Foundation supporting research grants (J. Baselga). L. He is supported by a DOD/CDMRP postdoctoral fellowship (BC093523).

## REFERENCES

1. Schneider BP, Winer EP, Foulkes WD, Garber J, Perou CM, Richardson A, et al. Triple-negative breast cancer: risk factors to potential targets. Clin Cancer Res. 2008; 14:8010–8. [PubMed: 19088017]
2. Tutt A, Robson M, Garber JE, Domchek SM, Audeh MW, Weitzel JN, et al. Oral poly(ADP-ribose) polymerase inhibitor olaparib in patients with BRCA1 or BRCA2 mutations and advanced breast cancer: a proof-of-concept trial. Lancet. 2010; 376:235–44. [PubMed: 20609467]
3. Fong PC, Boss DS, Yap TA, Tutt A, Wu P, Mergui-Roelvink M, et al. Inhibition of poly(ADP-ribose) polymerase in tumors from BRCA mutation carriers. N Engl J Med. 2009; 361:123–34. [PubMed: 19553641]
4. Farmer H, McCabe N, Lord CJ, Tutt AN, Johnson DA, Richardson TB, et al. Targeting the DNA repair defect in BRCA mutant cells as a therapeutic strategy. Nature. 2005; 434:917–21. [PubMed: 15829967]
5. Ashworth A. A synthetic lethal therapeutic approach: poly(ADP) ribose polymerase inhibitors for the treatment of cancers deficient in DNA double-strand break repair. J Clin Oncol. 2008; 26:3785–90. [PubMed: 18591545]
6. Lord CJ, Garrett MD, Ashworth A. Targeting the double-strand DNA break repair pathway as a therapeutic strategy. Clin Cancer Res. 2006; 12:4463–8. [PubMed: 16899589]
7. McCabe N, Turner NC, Lord CJ, Kluzek K, Bialkowska A, Swift S, et al. Deficiency in the repair of DNA damage by homologous recombination and sensitivity to poly(ADP-ribose) polymerase inhibition. Cancer Res. 2006; 66:8109–15. [PubMed: 16912188]
8. Johnson N, Li YC, Walton ZE, Cheng KA, Li D, Rodig SJ, et al. Compromised CDK1 activity sensitizes BRCA-proficient cancers to PARP inhibition. Nat Med. 2011; 17:875–82. [PubMed: 21706030]
9. Adimoolam S, Sirisawad M, Chen J, Thiemann P, Ford JM, Buggy JJ. HDAC inhibitor PCI-24781 decreases RAD51 expression and inhibits homologous recombination. Proc Natl Acad Sci U S A. 2007; 104:19482–7. [PubMed: 18042714]
10. Andre F, Job B, Dessen P, Tordai A, Michiels S, Liedtke C, et al. Molecular characterization of breast cancer with high-resolution oligonucleotide comparative genomic hybridization array. Clin Cancer Res. 2009; 15:441–51. [PubMed: 19147748]
11. Gewinner C, Wang ZC, Richardson A, Teruya-Feldstein J, Etemad-moghadam D, Bowtell D, et al. Evidence that inositol polyphosphate 4-phosphatase type II is a tumor suppressor that inhibits PI3K signaling. Cancer Cell. 2009; 16:115–25. [PubMed: 19647222]
12. Saal LH, Holm K, Maurer M, Memeo L, Su T, Wang X, et al. PIK3CA mutations correlate with hormone receptors, node metastasis, and ERBB2, and are mutually exclusive with PTEN loss in human breast carcinoma. Cancer Res. 2005; 65:2554–9. [PubMed: 15805248]
13. Nielsen TO, Hsu FD, Jensen K, Cheang M, Karaca G, Hu Z, et al. Immunohistochemical and clinical characterization of the basal-like subtype of invasive breast carcinoma. Clin Cancer Res. 2004; 10:5367–74. [PubMed: 15328174]
14. Wong KK, Engelman JA, Cantley LC. Targeting the PI3K signaling pathway in cancer. Curr Opin Genet Dev. 2010; 20:87–90. [PubMed: 20006486]
15. Kumar A, Fernandez-Capetillo O, Carrera AC. Nuclear phosphoinositide 3-kinase beta controls double-strand break DNA repair. Proc Natl Acad Sci U S A. 2011; 107:7491–6.
16. Kao GD, Jiang Z, Fernandes AM, Gupta AK, Maity A. Inhibition of phosphatidylinositol-3-OH kinase/Akt signaling impairs DNA repair in glioblastoma cells following ionizing radiation. J Biol Chem. 2007; 282:21206–12. [PubMed: 17513297]

17. Graeser M, McCarthy A, Lord CJ, Savage K, Hills M, Salter J, et al. A marker of homologous recombination predicts pathologic complete response to neoadjuvant chemotherapy in primary breast cancer. Clin Cancer Res. 2010; 16:6159–68. [PubMed: 20802015]
18. Burma S, Chen BP, Murphy M, Kurimasa A, Chen DJ. ATM phosphorylates histone H2AX in response to DNA double-strand breaks. J Biol Chem. 2001; 276:42462–7. [PubMed: 11571274]
19. Bartkova J, Horejsi Z, Koed K, Kramer A, Tort F, Zieger K, et al. DNA damage response as a candidate anti-cancer barrier in early human tumorigenesis. Nature. 2005; 434:864–70. [PubMed: 15829956]
20. Hans MA, Muller M, Meyer-Ficca M, Burkle A, Kupper JH. Overexpression of dominant negative PARP interferes with tumor formation of HeLa cells in nude mice: evidence for increased tumor cell apoptosis *in vivo*. Oncogene. 1999; 18:7010–5. [PubMed: 10597301]
21. Derose YS, Wang G, Lin YC, Bernard PS, Buys SS, Ebbert MT, et al. Tumor grafts derived from women with breast cancer authentically reflect tumor pathology, growth, metastasis and disease outcomes. Nat Med. 2011; 17:1514–20. [PubMed: 22019887]
22. Garcia-Garcia C, Ibrahim YH, Serra V, Calvo MT, Guzman M, Grueso J, et al. Dual mTORC1/2 and HER2 blockade results in antitumor activity in preclinical models of breast cancer resistant to anti-HER2 therapy. Clin Cancer Res. 2012; 18:2603–12. [PubMed: 22407832]
23. Gonzalez-Angulo AM, Ferrer-Lozano J, Stemke-Hale K, Sahin A, Liu S, Barrera JA, et al. PI3K pathway mutations and PTEN levels in primary and metastatic breast cancer. Mol Cancer Ther. 2011; 10:1093–101. [PubMed: 21490305]
24. Rogakou EP, Nieves-Neira W, Boon C, Pommier Y, Bonner WM. Initiation of DNA fragmentation during apoptosis induces phosphorylation of H2AX histone at serine 139. J Biol Chem. 2000; 275:9390–5. [PubMed: 10734083]
25. Lu C, Zhu F, Cho YY, Tang F, Zykova T, Ma WY, et al. Cell apoptosis: requirement of H2AX in DNA ladder formation, but not for the activation of caspase-3. Mol Cell. 2006; 23:121–32. [PubMed: 16818236]
26. Serra V, Scaltriti M, Prudkin L, Eichhorn PJ, Ibrahim YH, Chandarlapaty S, et al. PI3K inhibition results in enhanced HER signaling and acquired ERK dependency in HER2-overexpressing breast cancer. Oncogene. 2011; 30:2547–57. [PubMed: 21278786]
27. Chandarlapaty S, Sawai A, Scaltriti M, Rodrik-Outmezguine V, Grbovic-Huezo O, Serra V, et al. AKT inhibition relieves feedback suppression of receptor tyrosine kinase expression and activity. Cancer Cell. 2011; 19:58–71. [PubMed: 21215704]
28. Chaturvedi D, Gao X, Cohen MS, Taunton J, Patel TB. Rapamycin induces transactivation of the EGFR and increases cell survival. Oncogene. 2009; 28:1187–96. [PubMed: 19151764]
29. Jaspar Database. [cited 2011]. Available from: http://jaspar.cgb.ki.se
30. Sharrocks AD. The ETS-domain transcription factor family. Nat Rev Mol Cell Biol. 2001; 2:827–37. [PubMed: 11715049]
31. Baker KM, Wei G, Schaffner AE, Ostrowski MC. Ets-2 and components of mammalian SWI/SNF form a repressor complex that negatively regulates the BRCA1 promoter. J Biol Chem. 2003; 278:17876–84. [PubMed: 12637547]
32. Gelmon KA, Hirte HW, Robidoux A, Tonkin KS, Tischkowitz M, Swenerton K, et al. Can we define tumors that will respond to PARP inhibitors? A phase II correlative study of olaparib in advanced serous ovarian cancer and triple-negative breast cancer. J Clin Oncol. 2010; 28(suppl): 15s. abstr 3002.
33. Esteller M, Silva JM, Dominguez G, Bonilla F, Matias-Guiu X, Lerma E, et al. Promoter hypermethylation and BRCA1 inactivation in sporadic breast and ovarian tumors. J Natl Cancer Inst. 2000; 92:564–9. [PubMed: 10749912]
34. Powell, S. Homologous recombination defects found in all sub-types of sporadic breast cancer [abstract]; Proceedings of the 103rd Annual Meeting of the American Association for Cancer Research; Chicago, IL. Philadelphia (PA): AACR. 2012 Mar 31–Apr 4; 2012. Abstract nr MW11
35. Brenner JC, Ateeq B, Li Y, Yocum AK, Cao Q, Asangani IA, et al. Mechanistic rationale for inhibition of poly(ADP-ribose) polymerase in ETS gene fusion-positive prostate cancer. Cancer Cell. 2011; 19:664–78. [PubMed: 21575865]

36. Konishi H, Mohseni M, Tamaki A, Garay JP, Croessmann S, Karnan S, et al. Mutation of a single allele of the cancer susceptibility gene BRCA1 leads to genomic instability in human breast epithelial cells. Proc Natl Acad Sci U S A. 2011; 108:17773–8. [PubMed: 21987798]

37. Parker, JS.; Mullins, M.; Cheang, MC.; Leung, S.; Voduc, D.; Vickery, T., et al. Supervised risk predictor of breast cancer based on intrinsic subtypes.

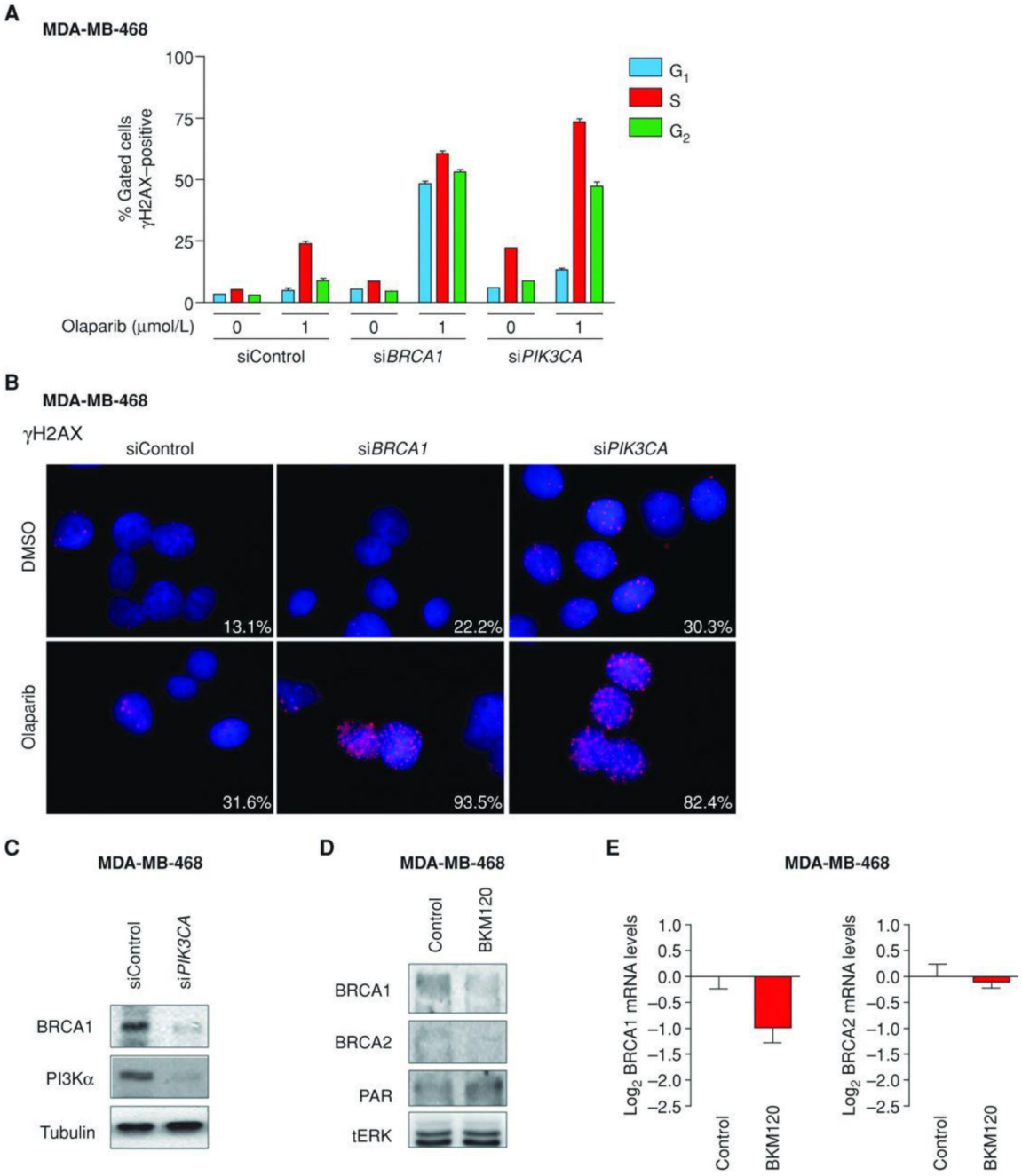


**Figure 1.**

BRCA downregulation and γH2AX staining following PI3K inhibition *in vitro*. **A,** fluorescence-activated cell-sorting (FACS) analysis showing staining of γH2AX during the 3 phases of the cell cycle ($G_1$, S, $G_2$) in MDA-MB-468 cells transfected with control, *BRCA1*, or *PIK3CA* siRNAs and treated with either dimethyl sulfoxide (DMSO) or 1 μmol/L olaparib. **B,** immunofluorescence of γH2AX in MDA-MB-468 cells transfected with control, *BRCA1*, or *PIK3CA* siRNAs and treated with either DMSO or 1 μmol/L of olaparib. Percentages of positive nuclei (10 foci or more per nucleus being considered

positive) from 10 fields per sample are indicated. **C,** Western blot analysis of cell lysates (7 days posttransfection) from MDA-MB-468 cells transfected with control or *PIK3CA* siRNAs using the indicated antibodies. Tubulin was used as loading control. **D,** Western blot analysis of lysates from MDA-MB-468 treated with BKM120 (750 nmol/L) for 7 days using the indicated antibodies. Total ERK (tERK) was used as a loading control. **E,** quantitative real-time PCR (qRT-PCR) measuring both *BRCA1* and *BRCA2* mRNA levels in MDA-MB-468 treated with BKM120. Measurements were normalized to *18S* mRNA levels and expressed as fold change compared with controls ($\log_2$ scale). Data are shown as mean ± SE of 3 independent replicates for each condition.

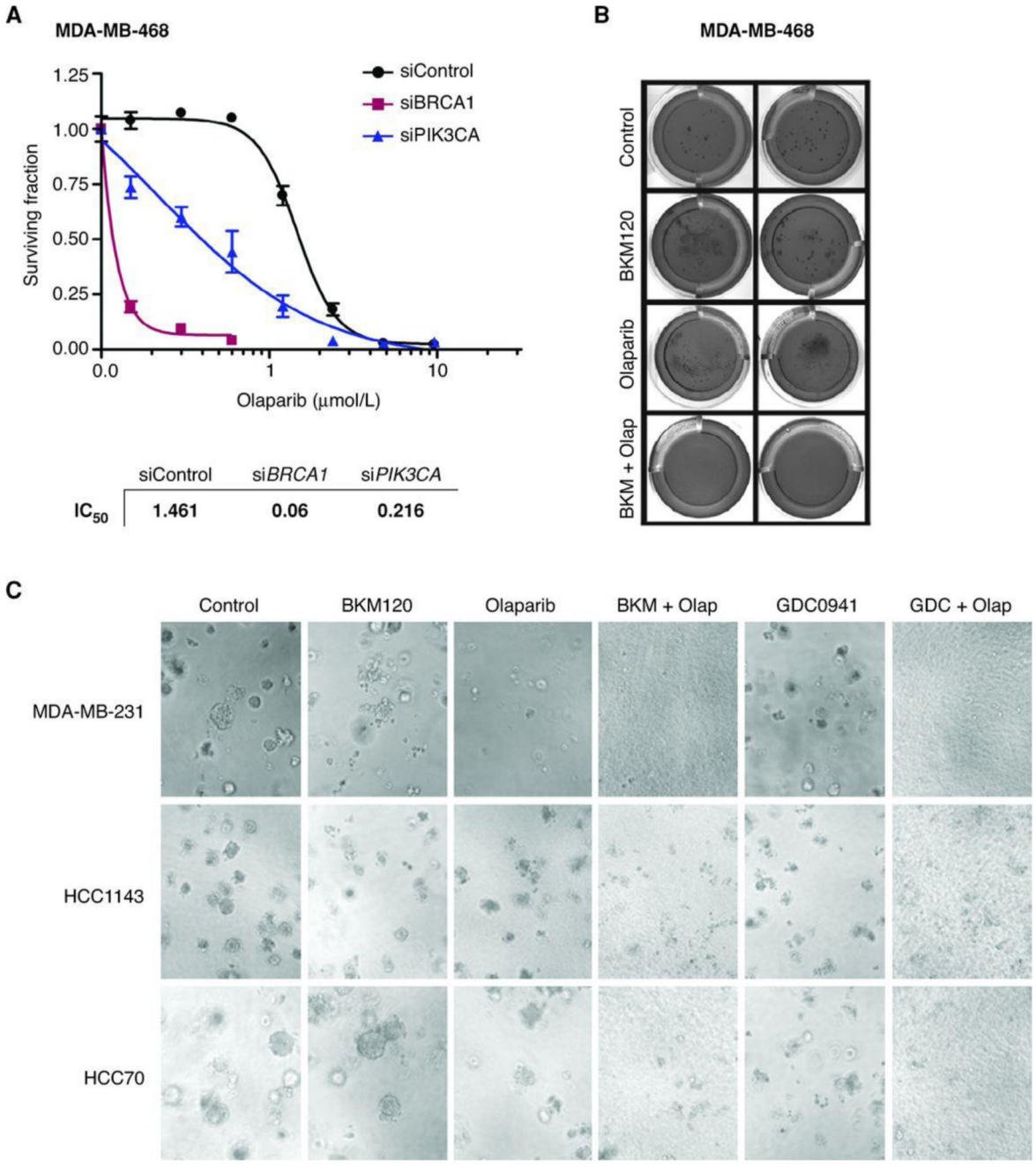


**Figure 2.**

Combined PI3K and PARP suppression *in vitro*. **A,** viability (assayed by Cell Titer-Glo) of MDA-MB-468 cells transfected with control, *BRCA1*, or *PIK3CA* siRNAs and treated with either dimethyl sulfoxide (DMSO) or olaparib for 7 days. $IC_{50}$ values were calculated using the GraphPad Prism program. **B,** MDA-MB-468 cells plated in anchorage-independent conditions treated with BKM-120 (750 nmol/L), olaparib (4 μmol/L), or the combination for 45 days, with weekly media changes. Cell colonies were stained with crystal violet. **C,** MDA-MB-231, HCC1143, and HCC70 cells plated in anchorage-dependent conditions

treated with BKM-120 (750 nmol/L), olaparib (4 μmol/L), GDC-0941 (500 nmol/L), or the combination for 7 days. Magnification, ×10.

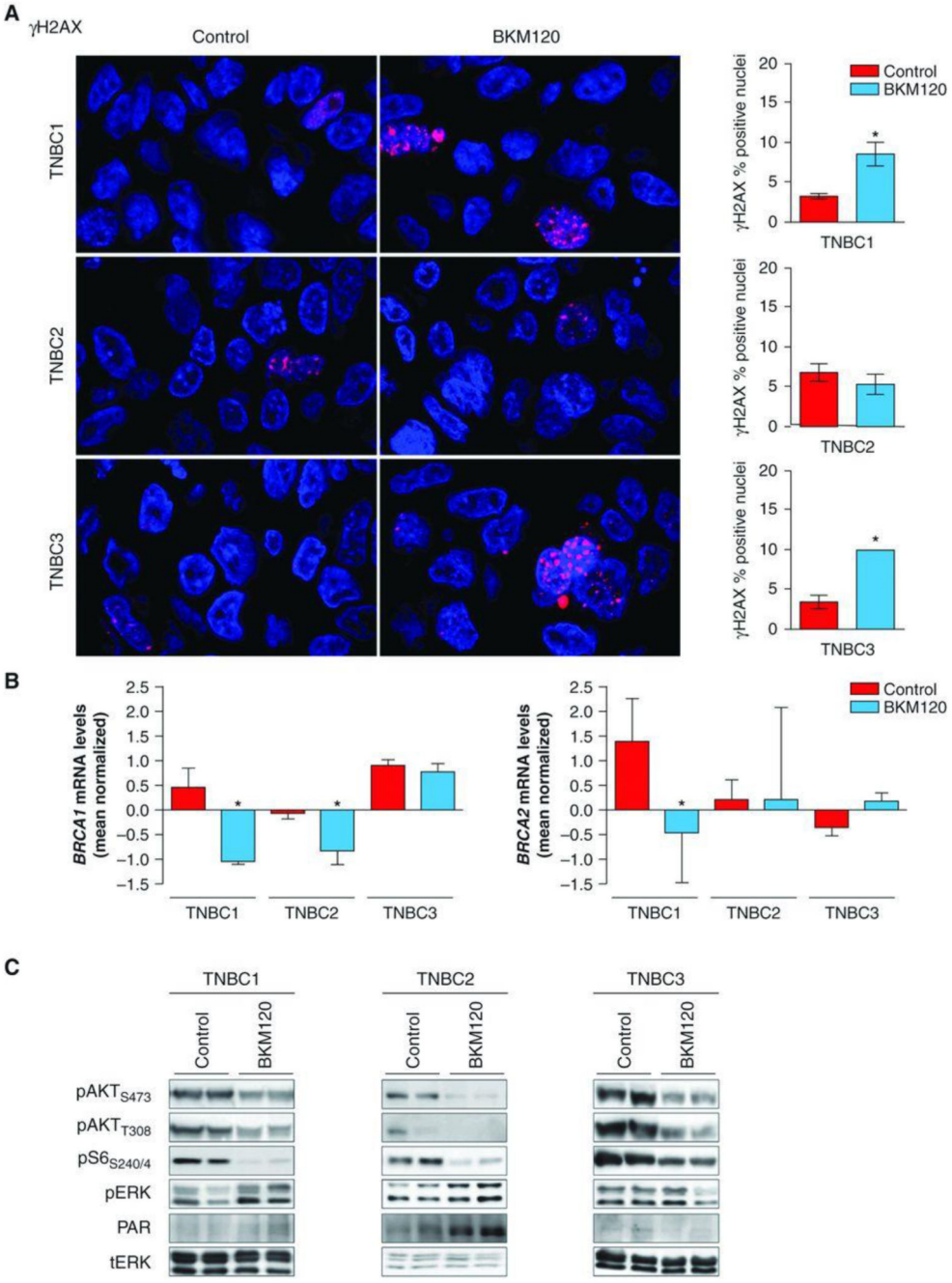


**Figure 3.**

γH2AX staining and BRCA downregulation following PI3K inhibition *in vivo*. **A,** representative immunofluorescence staining for γH2AX (red) comparing placebo versus BKM120-treated (27.5 mg/kg) TNBC xenografts. Nuclei are stained with DAPI (blue). Quantifications of γH2AX staining are from 6 different tumors for each condition. *, $P <$ 0.001. Magnification, ×20. **B,** qRT-PCR measuring both *BRCA1* and *BRCA2* mRNA levels of patient-derived TNBC1 and TNBC2 treated with BKM120. Measurements were normalized to *18S* mRNA levels and expressed as fold change compared with controls ($\log_2$

scale). Data are shown as mean ± SE of 3 independent replicates for each condition. *, $P < 0.001$. **C,** Western blot analysis of patient-derived xenografts of 2 independent tumors from different mice treated for 21 days with vehicle or BKM120 (27.5 mg/kg) using the indicated antibodies. Total ERK (tERK) is used as loading control.

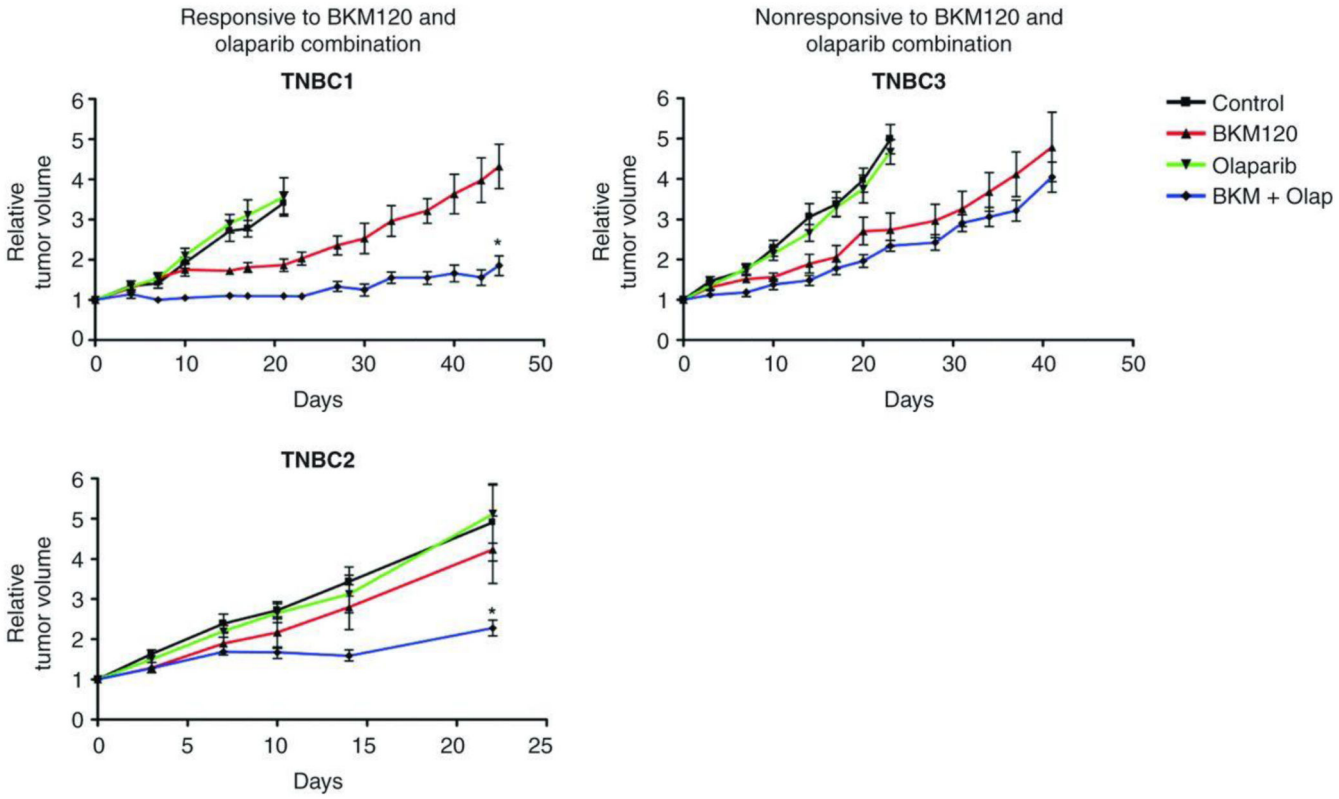


**Figure 4.**

Combined PI3K and PARP suppression *in vivo*. Tumor growth of TNBC1, TNBC2, and TNBC3 xenografts treated with vehicle control, BKM120 (27.5 mg/kg), olaparib (Olap; 50 mg/kg), or the combination of both agents. Relative tumor volumes are displayed as mean ± SE of a minimum of 6 tumors per arm. *, $P < 0.001$ combination versus BKM120 arm.

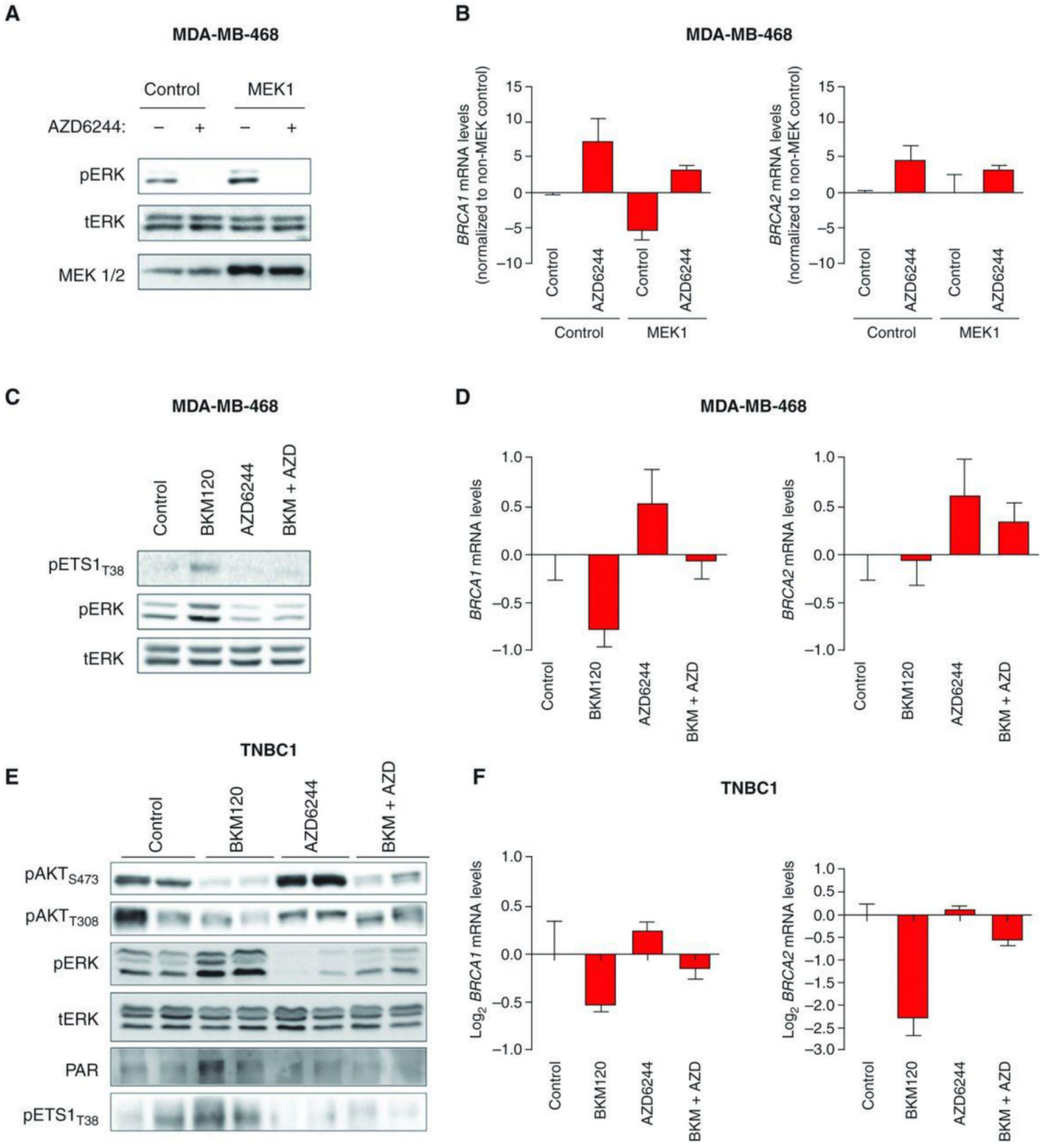


**Figure 5.**

ERK-dependent BRCA downregulation. **A,** Western blot analysis of protein lysates from MDA-MB-468 cells constitutively overexpressing control or MEK1 plasmids and treated with the MEK inhibitor AZD6244 (500 nmol/L) for 4 days using the indicated antibodies. Total ERK (tERK) is used as loading control. **B,** qRT-PCR measuring both *BRCA1* and *BRCA2* mRNA levels in MDA-MB-468-MEK1 cells treated with AZD6244. Measurements were normalized to 18S mRNA levels and expressed as fold change compared to controls ($\log_2$ scale). Data are shown as mean ± SE of 3 independent replicates for each condition. **C,**

Western blot analysis of protein lysates from MDA-MB-468 cells treated with BKM120 (750 nmol/L), AZD6244 (500 nmol/L), or the combination of both for 4 days using the indicated antibodies. Total ERK (tERK) is used as loading control. **D,** qRT-PCR measuring both *BRCA1* and *BRCA2* mRNA levels in MDA-MB-468 cells treated with BKM120 and AZD6244. Measurements were normalized to 18S mRNA levels and expressed as fold change compared with controls ($log_2$ scale). Data are shown as mean ± SE of 3 independent replicates for each condition. **E,** Western blot analysis of the indicated proteins in 2 independent TNBC1 tumors treated for 4 days with BKM120 (50 mg/kg), AZD6244 (10 mg/kg), or the combination of both. Total ERK (tERK) is used as loading control. **F,** qRT-PCR measuring both *BRCA1* and *BRCA2* mRNA levels in tumor grafts. Measurements were normalized to 18S mRNA levels and expressed as fold change compared with controls ($log_2$ scale). Data are shown as mean ± SE of 3 tumors for each condition.

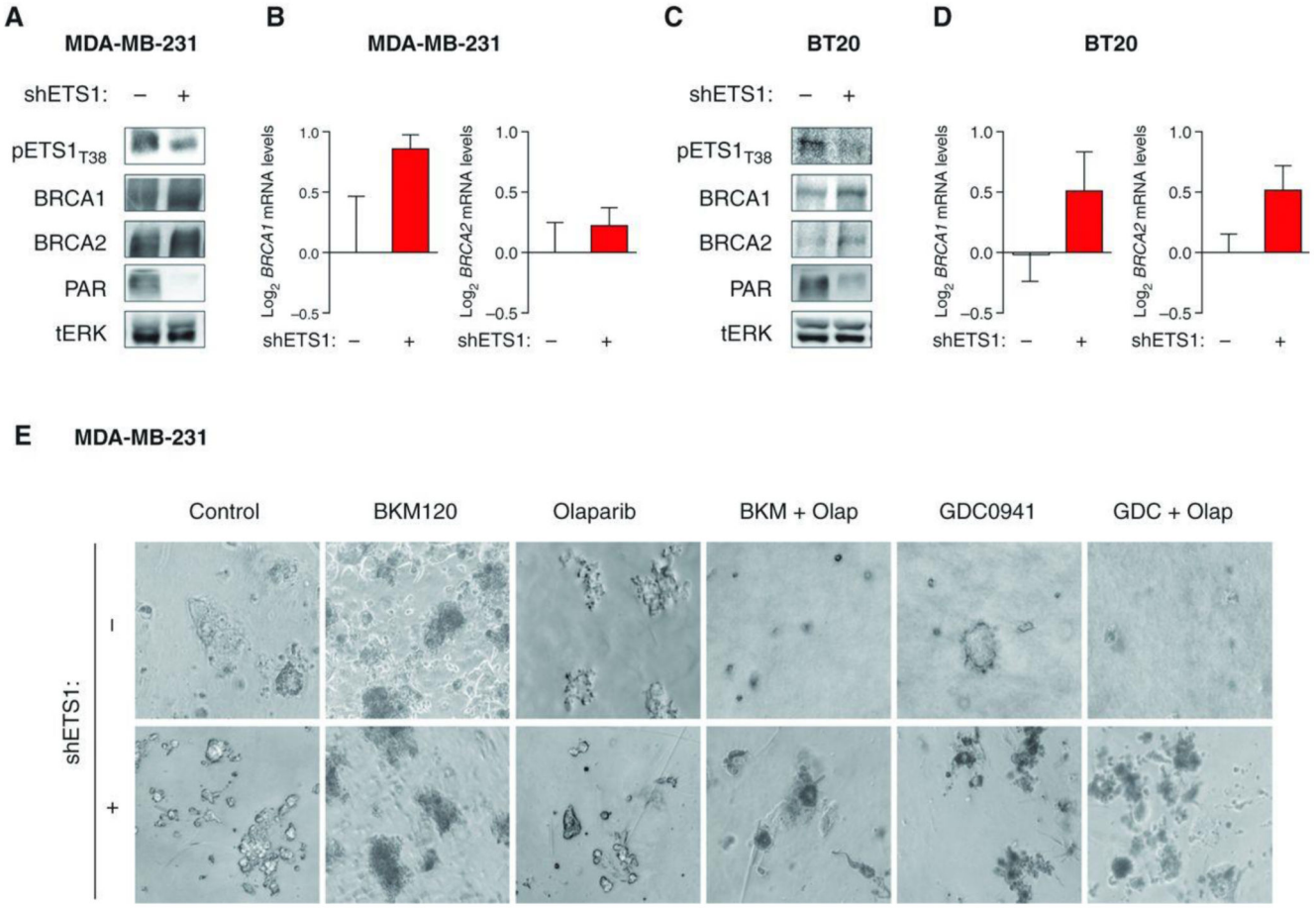


**Figure 6.**

ETS1 knockdown and resistance to the combination of BKM120 and olaparib. **A,** Western blot analysis of protein lysates from MDA-MB-231 shRNA-*ETS1*–infected cells treated with doxycycline (20 ng/mL) for 4 days using the indicated antibodies. Total ERK (tERK) is used as loading control. **B,** qRT-PCR measuring both *BRCA1* and *BRCA2* mRNA levels in MDA-MB-231-sh*ETS1* cells treated with doxycycline. Measurements were normalized to *18S* mRNA levels and expressed as fold change compared with controls ($\log_2$ scale). Data are shown as mean ± SE of 3 independent replicates for each condition. **C,** Western blot analysis of protein lysates from BT20 shRNA-*ETS1*–infected cells treated with doxycycline (20 ng/mL) for 4 days using the indicated antibodies. Total ERK (tERK) is used as loading control. **D,** qRT-PCR measuring both *BRCA1* and *BRCA2* mRNA levels in BT20-sh*ETS1* cells treated with doxycycline. **E,** MDA-MB-231-shETS1 cells plated in anchorage-dependent conditions were treated with/without doxycycline (20 ng/mL) and BKM-120 (750 nmol/L), olaparib (Olap; 4 μmol/L), GDC-0941 (500 nmol/L), or the combination for 14 days. Magnification, ×10.

## Table 1
## Characterization of TNBC patient–derived tumor xenografts

| Sample ID | Source | PTEN IHC (*H*-score) | *PIK3CA* status (MassArray) | *BRCA* status (Sanger) | PAM50 |
|---|---|---|---|---|---|
| TNBC1 | Metastatic | 0 | H1047R | Wild-type | Basal-like |
| TNBC2 | Metastatic | 0 | Wild-type | Wild-type | Basal-like/claudin-low[a] |
| TNBC3 | Primary | 0 | Wild-type | Wild-type | Basal-like |

NOTE: Expression of PTEN and *PIK3CA* or *BRCA1/2* mutational statuses of 3 tumor grafts derived from either primary or metastatic lesions of different patients with TNBCs. A minimum of 3 independent samples were used for PTEN quantification by immunohistochemistry. Molecular subtype analysis was conducted using PAM50 molecular analysis of Affymetrix microarrays.

Abbreviation: IHC, immunohistochemistry.

[a]Low estrogen receptor expression by IHC.